A MULTI-CURRENCY MODEL WITH FX VOLATILITY SKEW

VLADIMIR V. PITERBARG

Abstract. The paper develops a multi-currency model with FX skew for power-reverse dual-currency (PRDC) swaps, with a particular emphasis on model calibration to FX options across different maturities and strikes. Autonomous Markovian dynamics of the forward FX rate, exact for European options, are derived by the means of Dupire's approach. When combined with powerful skew averaging techniques, a fast and robust calibration method is developed. The impact of the FX skew on cancellable and knockout PRDC swaps is analyzed.

1. Introduction

Power-Reverse Dual-Currency (PRDC) swaps are by far the most widely traded and liquid cross-currency exotics. Continuing interest in these structures, driven by predominantly Japanese investors looking for higher yield, has resulted in large books of PRDCs being accumulated by most exotics dealers in the market. Large, concentrated exposures require sophisticated and robust models to risk-manage them properly. These demands have ensured that the modeling for PRDCs has received, and continues to receive, a significant share of attention by quantitative research departments in many banks.

PRDCs are essentially long-dated (30 years being quite typical) swaps with coupons that are options on the FX rate (most commonly a dollar-yen rate). They are often Bermuda-style callable, or have knockout provisions. PRDCs are exposed to the moves in the FX rate, and in the interest rates in both currencies. By now, most dealers have standardized on a three-factor modeling framework (see eg [SO02]), with the FX rate following a log-normal process, and the interest rates in the two currencies driven by one-factor Gaussian models. Keeping the number of factors to the minimum allows to use PDE-based methods for valuation, an essential requirement for large books. The choice of Gaussian assumptions for the interest rates and the log-normality for the FX rate has allowed for a very efficient, essentially closed-form, calibration to at-the-money options on the FX rate.

The assumption of lognormality for the FX rate, while technically very convenient, has little basis in reality. In fact, FX options exhibit a significant volatility skew (induced in longer-dated options, ironically, by dealers trying to hedge their PRDC positions). Moreover, the structure of PRDCs, epitomized in the typical choice of strikes for the coupons, as well as the callability/knockout features, makes them particularly sensitive to the FX volatility skew. Quantifying the FX skew exposure is only possible with a model that incorporates the FX skew. Building such a model is by no means trivial. While various mechanisms for including a skew in the model are well-known (local volatility, stochastic volatility and/or jumps), their applicability in the context of PRDC modeling is hindered by the same problem, namely that of calibration. Any particular skew-inducing mechanism is most typically imposed on the *instantaneous* FX rate. To calibrate to FX options, however, a *term* distribution of the forward FX rate to various expiries is required. The presence of stochastic interest rates makes the connection between the two particularly non-trivial. The problem is perhaps one of the most important current outstanding problems for quantitative

Date: February 7, 2005.

Key words and phrases. Power-reverse dual-currency notes, PRDC, FX volatility skew, three-factor model, multi-currency model.

I would like to thank Jesper Andreasen and Leif Andersen for thoughtful comments.

research departments worldwide, yet the literature on the subject is all but non-existent[1], except for some interesting results presented at conferences ([Bal05]).

In this paper, we build a cross-currency model that incorporates FX volatility smiles. We stay in the context of local volatility models, which allows us to avoid introducing any more stochastic factors, thus keeping the speed and accuracy of valuation the same as in the "standard", log-normal model. Most of the focus is given to the problem of calibrating FX options for various maturities and strikes simultaneously. The main contribution of the paper is a calibration procedure that can be performed essentially *instantaneously*. The procedure is obtained by combining our recently developed techniques of skew averaging (see [Pit05a], [Pit05b]) with a derived Markovian representation of the dynamics of the forward FX rate that is exact for European options.

The paper is organized as follows. The model is defined in Section 2, the questions of valuation are addressed in Section 3, and an overview of the calibration problem is given in Section 4. The process for the forward FX rate is derived in Section 5. The Markovian representation of the forward FX rate is derived in Section 6. Skew averaging results are applied to the Markovian representation of the forward FX rate in Section 7, where the main FX option approximation result, Theorem 7.2, is obtained. The scheme for calibrating the model to FX options of different expiries and strikes, based on the approximation results from previous sections, is developed in Section 8. Fit to market is discussed in Section 9. The quality of approximations and calibration is tested in Section 10. The impact of FX volatility skew on various flavors of PRDCs is studied in Section 11. Section 12 concludes the paper.

2. The model

An economy with two currencies, "domestic" and "foreign", is considered. Let $\mathbf{P}$ be the domestic risk-neutral measure. Let $P_i(t,T)$, $i=d,f$, be the prices, in their respective currencies, of the domestic and foreign zero-coupon discount bonds. Also let $r_i(t)$, $i=d,f$, be the short rates in the two currencies. Let $S(t)$ be the spot FX rate, expressed in the units of domestic currency per one unit of the foreign currency. For future purposes, the forward FX rate (the break-even rate for a forward FX transaction) is denoted by $F(t,T)$, with the well-known relationship

$$F(t,T)=\frac{P_f(t,T)}{P_d(t,T)}S(t) \tag{2.1}$$

following from no-arbitrage arguments.

The following model is considered,

$$\begin{aligned} dP_d(t,T)/P_d(t,T) &= r_d(t)\,dt+\sigma_d(t,T)\,dW_d(t),\\ dP_f(t,T)/P_f(t,T) &= r_f(t)\,dt-\rho_{fS}\sigma_f(t,T)\gamma(t,S(t))\,dt+\sigma_f(t,T)\,dW_f(t),\\ dS(t)/S(t) &= (r_d(t)-r_f(t))\,dt+\gamma(t,S(t))\,dW_S(t), \end{aligned} \tag{2.2}$$

where $(W_d(t),W_f(t),W_S(t))$ is a Brownian motion under $\mathbf{P}$ with the correlation matrix

$$\begin{pmatrix} 1 & \rho_{df} & \rho_{dS}\\ \rho_{df} & 1 & \rho_{fS}\\ \rho_{dS} & \rho_{fS} & 1 \end{pmatrix}$$

(note the "quanto" drift adjustment for $dP_f(t,T)$ arising from changing the measure from the foreign risk-neutral to the domestic risk neutral). Gaussian dynamics for the rates are specified,

$$\sigma_i(t,T)=\sigma_i(t)\int_t^T e^{-\int_t^s \varkappa_i(u)du}ds,\quad i=d,f, \tag{2.3}$$

[1]While some banks are known to have introduced FX skews and smiles into cross-currency models, their methods for doing so have not been put in the public domain.

with $\sigma_d(t)$, $\sigma_f(t)$, $\varkappa_d(t)$, $\varkappa_f(t)$ deterministic functions. The FX skew in the model is imposed via the local volatility function $\gamma(t,x)$. The "standard" Gaussian framework, as developed in eg [DH97], is recovered by choosing the function $\gamma(t,x)$ that is independent of x, $\gamma(t,x)=\gamma(t)$. For the stability of calibration, it is essential to use a parametric form of the local volatility function. The following parametrization is used,

$$\gamma(t,x)=\nu(t)\left(\frac{x}{L(t)}\right)^{\beta(t)-1}, \tag{2.4}$$

where $\nu(t)$ is the relative volatility function, $\beta(t)$ is a time-dependent constant elasticity of variance (CEV) parameter and $L(t)$ is a time-dependent scaling constant ("level"). Our choice of the parametric form is motivated by well-known problems (see [AA02]) with the dynamics, and subsequent hedging performance, of models with "U-shaped" local volatility functions. Among more "flat" functions, most choices are essentially equivalent, with the CEV specification being slightly more technically convenient.

3. Valuation

Before discussing the issues of calibration, let us explain why the choices made in specifying the model (2.2) make it particularly simple to use for cross-currency exotics (such as PRDCs). The volatility structures of zero-coupon discount bonds defined by (2.3) can be recognized as arising from the one-factor Gaussian HJM model (sometimes called the Hull-White, or extended Vasicek, model). A one-factor model admits a Markovian representation in the short rate. In particular, the following holds true,

$$dr_i(t)=(\theta_i(t)-\varkappa_i(t)\,r_i(t))\,dt-\sigma_i(t)\,dW_i(t),\quad i=d,f,$$

(under the respective risk-forward measures), where $\theta_i(t)$ are known in closed form (see eg [BM01]). Moreover, zero-coupon discount bonds can be written as deterministic functions of the short rates. Hence, the model (2.2) admits a Markovian representation in three variables[2], $(r_d(\cdot), r_f(\cdot), S(\cdot))$. Let $V=V(t,r_d,r_f,S)$ be the value of a security (such as a PRDC) at time t, given the state variables. Then this function satisfies the following PDE

$$\begin{aligned}
&V_t+(\theta_d(t)-\varkappa_d(t)\,r_d)\,V_{r_d}\\
&+\left(\theta_f(t)+\rho_{fS}\sigma_f(t)\,\gamma(t,S(t))-\varkappa_f(t)\,r_d\right)V_{r_f}\\
&+(r_d-r_f)\,SV_S\\
&+\frac{1}{2}\sigma_d^2(t)\,V_{r_dr_d}+\frac{1}{2}\sigma_f^2(t)\,V_{r_fr_f}+\frac{1}{2}\gamma^2(t,S)\,S^2V_{SS}\\
&+\rho_{df}\sigma_d(t)\,\sigma_f(t)\,V_{r_dr_f}-\rho_{dS}\sigma_d(t)\,\gamma(t,S)\,SV_{r_dS}-\rho_{fS}\sigma_f(t)\,\gamma(t,S)\,SV_{r_fS}\\
&=r_dV.
\end{aligned}$$

This PDE in three space dimensions is most efficiently solved by utilizing a level-splitting scheme, such as an ADI scheme from [CS88].

4. Overview of calibration

Before a model can be used for valuation, its parameters need to be chosen to match market-observable prices of related securities. The parameters defining the volatility structures of interest rates in both currencies, ie the functions $\sigma_d(t)$, $\sigma_f(t)$, $\varkappa_d(t)$, $\varkappa_f(t)$, are typically chosen to match European swaption values in the respective currencies. Methods for doing this are well-known from (single-currency) interest rate modeling literature and are covered elsewhere (see eg [BM01]). The correlation parameters ρ_{ij}, $i,j=d,f,S$, are typically chosen either by historical estimation, or from

[2]Note that different choices of state variables are available, with some more technically convenient than the others. We use the most obvious choice.

occasionally-observed prices of "quanto" interest rate contracts (payoffs made in domestic currency but linked to rates in foreign currency). Of particular importance to PRDCs is how to calibrate the volatility function of the FX rate $\gamma(t,x)$. Options on the FX rate are traded across a wide range of maturities and strikes; this is the information to which $\gamma(t,x)$ should be calibrated. For PRDCs and most other cross-currency derivatives, it is impossible to pick a particular strike, or a particular maturity, of an FX option "relevant" for the security in question. Nor can cancellable/knockout PRDCs be decomposed into simple FX options. Hence, the volatility function $\gamma(t,x)$ needs to be calibrated to prices of all available FX options across maturities and strikes.

5. Forward FX rate

To be able to calibrate the model to options on the FX rate, values of such options in the model (2.2) need to be derived. A call option on the FX rate with strike K and maturity T pays $(S(T)-K)^+$ at time T, and its value at time 0 is equal to

$$c(T,K)=\mathbf{E}_0\left(e^{-\int_0^T r_d(s)\,ds}\left(S(T)-K\right)^+\right).$$

While the dynamics of the spot FX rate is complex, the dynamics of the forward FX rate are less so, owning to the fact that the forward FX rate is a martingale under the corresponding domestic forward measure. Moreover, switching to the forward measure leads to decoupling of discounting from the expected value calculations. Hence, it is convenient to rewrite the value of an option in terms of the forward FX rate,

$$c(T,K)=P_d(0,T)\,\mathbf{E}_0^T\left(\left(F(T,T)-K\right)^+\right),$$

and study the dynamics of $F(t,T)$ under the domestic T-forward measure $\mathbf{P}^T$ (the measure for which $P_d(\cdot,T)$ is a numeraire). The following result is obtained.

Proposition 5.1. *The forward FX rate $F(t,T)$ follows the dynamics*

$$dF(t,T)/F(t,T)=\sigma_f(t,T)\,dW_d^T(t)-\sigma_d(t,T)\,dW_d^T(t)+\gamma\left(t,F(t,T)D(t,T)\right)dW_S^T(t), \tag{5.1}$$

where $\left(W_d^T(t),W_f^T(t),W_S^T(t)\right)$ is a three-dimensional Brownian motion under the domestic T-forward measure. Moreover, there exists $dW_F(t)$, a Brownian motion under the domestic T-forward measure $\mathbf{P}^T$, such that

$$\frac{dF(t,T)}{F(t,T)}=\Lambda\left(t,F(t,T)D(t,T)\right)dW_F(t), \tag{5.2}$$

where

$$\begin{aligned}\Lambda(t,x)&=\left(a(t)+b(t)\,\gamma(t,x)+\gamma^2(t,x)\right)^{1/2},\\ a(t)&=\left(\sigma_f(t,T)\right)^2+\left(\sigma_d(t,T)\right)^2-2\rho_{df}\sigma_f(t,T)\,\sigma_d(t,T),\\ b(t)&=2\rho_{fS}\sigma_f(t,T)-2\rho_{dS}\sigma_d(t,T),\end{aligned}$$

and

$$D(t,T)\triangleq\frac{P_d(t,T)}{P_f(t,T)}.$$

Proof. The equation (5.1) is obtained by applying Ito's lemma to (2.1) and using the fact that $dF(t,T)$ is a martingale under the domestic T-forward measure. Denoting

$$dW_F=\frac{1}{\Lambda\left(t,F(t,T)D(t,T)\right)}\left(\sigma_f(t,T)\,dW_d^T(t)-\sigma_d(t,T)\,dW_d^T(t)+\gamma\left(t,F(t,T)D(t,T)\right)dW_S^T(t)\right), \tag{5.3}$$

the equation (5.2) follows from (5.1). The fact that W_F is a Brownian motion under $\mathbf{P}^T$ is established by computing the quadratic variation of dW_F from (5.3).

∎

Remark 5.1. *If $\gamma(t,x)$ is a function of time t only, $\gamma(t,x)=\gamma(t)$, then the diffusion coefficient for dF/F in (5.1) is in fact a deterministic function of time. In this case, $F(T,T)$ is lognormally distributed,*

$$\log F(t,T) \sim \mathcal{N}\left(-\sigma_F^2(T)\,T/2, \sigma_F(T)\sqrt{T}\right),$$
$$\sigma_F(T) = \left(\frac{1}{T}\int_0^T \left(a(t)+b(t)\gamma(t)+\gamma^2(t)\right)\,dt\right)^{1/2}.$$

In particular, FX options can be valued using the Black formula. Inversely, the function $\gamma(\cdot)$ can be implied from the FX option prices by solving a system of equations

$$\sigma_F(T_n) = \sigma_n^*, \quad n=1,\ldots,N,$$

for a collection of maturities $\{T_n\}_{n=1}^N$, where $\{\sigma_n^*\}_{n=1}^N$ are market-implied Black volatilities of FX options of given maturities (and strikes, one per maturity).

While in the case of $\gamma(t,x)$ not depending on x the term distribution of $F(\cdot,T)$ is easy to identify, this is not the case in the general case. Not only the diffusion coefficient of dF/F depends on F, it also depends on $D(t,T)$, another stochastic variable. In what follows we reduce the complexity of the diffusion coefficient step by step, ultimately bringing it into a recognizable form.

6. Markovian representation for forward FX rate

The first step in simplifying the dynamics of the forward FX rate is "closing out" the SDE for F, by which we mean writing the SDE in a Markovian form, a form that contains F as the only stochastic variable. The simplest "naive" approach to this would be to replace $D(t,T)$ in (5.2) with its "along the forward" deterministic approximation,

$$D(t,T) \approx D_0(t,T), \tag{6.1}$$
$$D_0(t,T) = \frac{P_d(0,t,T)}{P_f(0,t,T)},$$

where $P_i(s,t,T)$, $i=d,f$, are forward prices of corresponding zero-coupon discount bonds. This approach, in addition to being rather ad-hoc, also produces approximations of low accuracy. Instead, we derive an autonomous representation of the forward FX rate process that is *exact* for European options. The derivation uses Dupire's formula and is inspired by [**?**]. The same representation is used in [ABOBF02] as a starting point to derive an expression for the volatility of an index from volatilities of its components.

In what follows $T>0$, the settlement date of the FX forward rate, is fixed. Let us extend the definition of options being considered to include expiries before the settlement date of the FX forward, and define

$$c(t,T,K) = P_d(0,t)\,\mathbf{E}_0^T\left((F(t,T)-K)^+\right). \tag{6.2}$$

Consider the problem of finding a function $\tilde{\Lambda}(t,x)$ such that, in the model

$$\frac{dF(t,T)}{F(t,T)} = \tilde{\Lambda}(t,F(t,T))\,dW_F(t), \tag{6.3}$$

the values of European options $\{c(t,T,K)\}$ for all t,K, $0<t\le T$, $0\le K<\infty$, *match exactly* the values of the same options in the original model (2.2) (or, equivalently, (5.2)). This is done in the

spirit of Dupire's approach, as the values of options $\{c(t,T,K)\}$ (in the model (2.2)) are considered to be given, and the local volatility $\tilde{\Lambda}(t,x)$ is being determined from them.

The following theorem derives such a local volatility function in terms of model's parameters. The resulting SDE is called the "Markovian representation" of the original one.

Theorem 6.1. *The local volatility function $\tilde{\Lambda}(t,x)$ for which the values of all European options $\{c(t,T,K)\}_{t,K}$ in the model (6.3) are the same as in the model (2.2) is given by*

$$\tilde{\Lambda}^2(t,x) = \mathbf{E}_0^T\left(\Lambda^2(t,F(t,T)D(t,T))\middle|F(t,T)=x\right).$$

The proof of the theorem is given in Appendix A. The result is very intuitive – the Markovian dynamics is defined by the diffusion coefficient that is the expected value of the original diffusion coefficient conditioned on the underlying. We emphasize that the result is exact for European options and, hence, all derivatives with European-style payoffs.

In the next corollary, the theorem is used to derive an approximation to the dynamics of the forward FX rate. The proof is in Appendix B.

Corollary 6.2. *For the purposes of European option pricing, the dynamics of the forward FX rate $F(\cdot,T)$ under the measure $\mathbf{P}^T$ are approximately given by*

$$\frac{dF(t,T)}{F(t,T)} = \hat{\Lambda}(t,F(t,T))\,dW_F(t), \tag{6.4}$$

where

$$\begin{aligned}
\hat{\Lambda}(t,x) &= \left(a(t)+b(t)\hat{\gamma}(t,x)+\hat{\gamma}^2(t,x)\right)^{1/2},\\
\hat{\gamma}(t,x) &= \nu(t)\left(x\frac{D_0(t,T)}{L(t)}\right)^{\beta(t)-1}\left(1+(\beta(t)-1)r(t)\left(\frac{x}{F(0,T)}-1\right)\right),\\
r(t) &= \frac{\int_0^t \chi_{Z,F}(s)\,ds}{\int_0^t \chi_{F,F}(s)\,ds},
\end{aligned}$$

and

$$\begin{aligned}
\chi_{Z,F}(t) &= -a(t) - \frac{b(t)}{2}\gamma(t,F(0,T)D_0(t,T)),\\
\chi_{F,F}(t) &= a(t)+b(t)\gamma(t,F(0,T)D_0(t,T))+\gamma^2(t,F(0,T)D_0(t,T)).
\end{aligned} \tag{6.5}$$

Remark 6.1. *Had we used the simplistic approximation (6.1), the corresponding formula would simply be*

$$\hat{\gamma}(t,x) = \nu(t)\left(x\frac{D_0(t,T)}{L(t)}\right)^{\beta(t)-1}.$$

Clearly, accounting for the stochastic nature of $D(t,T)$ introduced an adjustment to the slope of the local volatility function $\hat{\gamma}(t,x)$ around the forward $x=F(0,T)$. The size of the correction depends on $r(t)$, which can be interpreted as a "regression coefficient" between $F(\cdot,T)$ and $D(\cdot,T)$. In fact, drawing an analogy with stochastic volatility models (with $D(\cdot,T)$ playing the role of the stochastic volatility), we can expect an adjustment to the curvature of the volatility smile resulting from the stochasticity in $D(\cdot,T)$ as well. In the approximation developed in the corollary, this effect is ignored.

The corollary derives an "autonomous" equation for $F(\cdot,T)$. It is a one-dimensional SDE with the diffusion coefficient given by a local volatility function $\hat{\Lambda}(t,x)$. Prices of options on $F(T,T)$ can in principle now be computed in a one-dimensional PDE (a significant reduction of effort from a three-dimensional one!) However, an even faster method is possible. It is developed next.

7. Skew averaging

Significant advances in deriving closed-form approximations to option prices in models with time-dependent local volatility (and stochastic volatility) parameters have been achieved recently, see [Pit05a], [Pit05b]. With the approach of "parameter averaging", time-dependent parameters are replaced with "effective", time-constant ones, thus allowing to relate model and market parameters directly without actually performing any option calculations. The next step in simplifying the equation for the forward FX rate is based on the following generic result.

Proposition 7.1. *Let $X(t)$ be a stochastic process defined by*

$$dX(t) = g(t, X(t))\, dW(t), \quad X(0) = X_0,$$

Then the distribution of $X(T)$ is well-approximated by the distribution of $Y(T)$, where the stochastic process $Y(t)$ is defined by

$$dY(t) = \sigma(t)\, \bar{g}(Y(t))\, dW(t), \quad Y(0) = X_0,$$

and the functions $\sigma(t)$, $\bar{g}(y)$ are such that

$$\begin{aligned} \sigma(t) &= g(t, X_0), \\ \bar{g}(X_0) &= 1, \\ \frac{\partial}{\partial x}\bar{g}(x)\Big|_{x=X_0} &= \int_0^T w(t)\, \frac{\frac{\partial}{\partial x} g(t,x)\big|_{x=X_0}}{g(t, X_0)} dt, \end{aligned}$$

and the weights $w(t)$ in the last equation are given by

$$w(t) = \frac{u(t)}{\int_0^T u(t)\, dt}, \quad u(t) = g^2(t, X_0) \int_0^t g^2(s, X_0)\, ds.$$

A generalization of this proposition is proved (in the small-slope asymptotic expansion sense) in [Pit05a]. Its meaning is transparent – a time-dependent local volatility function $g(t,x)$ can be replaced with a time-constant one $\bar{g}(x)$ if the latter has the slope at $x = X_0$ which is a weighted average of time-dependent slopes of $g(t,x)$ with given weights.

Applying the proposition to the forward FX rate driven by (6.4), the following result is obtained (see Appendix C for the proof).

Theorem 7.2. *To value options on the FX rate with maturity T, the forward FX rate can be approximated by the following SDE*

$$dF(t,T) = \hat{\Lambda}(t, F(0,T)) \left(\delta_F F(t,T) + (1-\delta_F) F(0,T)\right) dW_F(t),$$

where

$$\begin{aligned} \delta_F &= 1 + \int_0^T w(t)\, \frac{b(t)\, \eta(t) + 2\hat{\gamma}(t, F(0,T))\, \eta(t)}{2\hat{\Lambda}^2(t, F(0,T))}\, dt, \\ \eta(t) &= \hat{\gamma}(t, F(0,T))\, (1 + r(t))\, (\beta(t) - 1), \\ w(t) &= \frac{u(t)}{\int_0^T u(t)\, dt}, \\ u(t) &= \hat{\Lambda}^2(t, F(0,T)) \int_0^t \hat{\Lambda}^2(s, F(0,T))\, ds. \end{aligned} \tag{7.1}$$

In particular, $F(\cdot,T)$ follows a standard displaced-diffusion SDE with the skew parameter δ_F. The value $c(T,K)$ of a call option on the FX rate with maturity T and strike K is equal to

$$c(T,K) = P_d(0,T)\, c_{\text{Black}}\left(\frac{F(0,T)}{\delta_F}, K + \frac{1-\delta_F}{\delta_F}F(0,T), \sigma_F\delta_F, T\right), \tag{7.2}$$

$$\sigma_F = \left(\frac{1}{T}\int_0^T \hat{\Lambda}^2(t, F(0,T))\, dt\right)^{1/2}, \tag{7.3}$$

where $c_{\text{Black}}(F,K,\sigma,T)$ is the Black formula value for a call option with forward F, strike K, volatility σ, and time to maturity T.

This theorem fully resolves the problem of approximately pricing options on the FX rate in the cross-currency model (2.2). For a given expiry T and strike K, the pricing formula (7.2) is used with the "effective" volatility of the forward FX rate σ_F defined by (7.3), and the "effective" skew of the forward FX rate δ_F given by (7.1). In the next section, we examine how to build a calibration scheme based on these formulas.

8. Calibration

Let us assume that maturities

$$0 = T_0 < T_1 < \cdots < T_N$$

are given, and the model (2.2) is to be calibrated to the market prices of options on the FX rate with maturities $\{T_n\}_{n=1}^N$. In view of the parametrization (2.4), it essentially means determining the time-dependent functions $\nu(t)$ and $\beta(t)$ for $t \in [0, T_N]$ (the function $L(t)$ is chosen from the outset; the choice $L(t) = F(0,t)$, $t \geq 0$, is particularly convenient). Without loss of generality, the functions $\nu(t)$, $\beta(t)$ can be assumed piece-wise constant between the maturities,

$$\begin{aligned}\nu(t) &= \sum_{n=1}^N \nu_n \cdot 1_{(T_{n-1},T_n]}(t),\\ \beta(t) &= \sum_{n=1}^N \beta_n \cdot 1_{(T_{n-1},T_n]}(t).\end{aligned}$$

In Theorem 7.2, forward FX rates are approximated by a displaced-diffusion process. Thus, it is natural to express the market prices of FX options in terms of the displaced-diffusion model. In practice it means that for each maturity T_n, a *market* volatility σ_n^* and a *market* skew parameter δ_n^* are chosen so that the market prices of FX options with expiry T_n across a collection of strikes[3] are well-matched by the displaced-diffusion model of the form

$$dF(t,T) = \sigma_n^*\left(\delta_n^* F(t,T) + (1-\delta_n^*)F(0,T)\right) dW_F(t), \quad n = 1,\ldots,N.$$

Once the market prices are expressed in terms of $\{(\sigma_n^*, \delta_n^*)\}_{n=1}^N$, the problem of model calibration can be reformulated as follows.

> Find model parameters $\{(\nu_n, \beta_n)\}_{n=1}^N$ such that "effective" volatility $\sigma_F = \sigma_F(T_n)$ and "effective" skew $\delta_F = \delta_F(T_n)$, computed for each expiry T_n from $\{(\nu_k, \beta_k)\}_{k=1}^N$ according to the formulas (7.3), (7.1) in Theorem 7.2, match the market-implied values $\{(\sigma_n^*, \delta_n^*)\}_{n=1}^N$.

[3]FX options of different strikes may not necessarily be well-matched the displaced-diffusion model. We disucss this issue in upcoming sections.

This is essentially an algebraic root-search problem, and a fairly easy one to solve. Moreover, by analyzing the formulas (7.3), (7.1) and the ones they depend on, it becomes clear that the calculations can be organized so that the problem can be split into N sequential problems, each one involving only a two-dimensional root search. In particular, $\sigma_F(T_1)$, $\delta_F(T_1)$ depend on ν_1, β_1 only. Hence, they can be determined from the equations

$$\begin{aligned}\sigma_F(T_1) &= \sigma_1^*,\\ \delta_F(T_1) &= \delta_1^*.\end{aligned}$$

The values $\sigma_F(T_2)$, $\delta_F(T_2)$ depend on ν_1, ν_2, β_1, β_2 only. The values of ν_1, β_1 determined on the first step can be used, thus reducing the problem again to a two-dimensional root search for ν_2, β_2. This procedure can be repeated recursively until all $\{(\nu_k, \beta_k)\}_{k=1}^N$ are found. In practice, the calibration takes fractions of a second on a computer.

9. Quality of fit and future directions

FX volatility smiles generated by the model (2.2) are well-approximated by displaced-diffusion type smiles, as demonstrated above. A displaced-diffusion model, compared to the log-normal one, adds another parameter to control the shape of the volatility smile. In particular, the skew parameter δ allows to change its slope. While this is a significant improvement over the log-normal model (where the slope of the smile cannot be changed), it may not be enough to match the market-observed FX volatility smile perfectly. In particular, market smiles often have some curvature to them, a feature that cannot be reproduced in the model developed. Typical examples can be seen in Figures 4, 5, 6. While the differences between the smiles that the model can generate and the market smiles are mostly small, one may wonder if the quality of fit can be improved. There are two routes one may take in this regard.

The first approach is to stay within the framework developed in this paper, but change the parametrization of the local volatility function $\gamma(t,x)$ in (2.4). In particular, if $\gamma(t,x)$ is chosen from a parametric family with more curvature, it will naturally be reflected in more curvature in FX volatility smiles produced by the model. While this course is appealing, there are some caveats. First, as already mentioned, modeling significantly-convex volatility smiles within a local volatility framework is generally a bad idea, because of the problems with the dynamics of the smile in such models (it gets inverted in certain future states in the world, something never observed in the real world). Second, on the technical side, the performance of the skew averaging method in Proposition 7.1 deteriorates for more convex local volatility functions. Hence, the method may have to be extended.

The second approach is to enrich the model by adding a smile generation mechanism that is more capable of producing significantly-convex volatility smiles. For example, a suitable extension of the model with the stochastic volatility imposed on the FX rate will ultimately provide the most satisfying framework for long-dated FX volatility smile modeling. This approach is not without its own difficulties, however. First, adding stochastic volatility will add an extra state variable to the model, making the PDE method less suitable for valuation. Second, calibration procedures will likely to be significantly more complicated and less stable.

Both approaches are feasible, and are left for future work to be explored. But even with less-than-perfect match to the volatility smiles, the model is a significant advance in PRDC modeling. Not only does it provide a much better fit to market FX volatilities than the "standard" log-normal version, it also allows to directly measure the impact of various volatility smile assumptions on prices of securities such as cancellable and knockout PRDCs, something that is simply not possible with a model without smiles. We will discuss some of these findings in future sections.

Expiry	Strike 1	Strike 2	Strike 3	Strike 4	Strike 5	Strike 6	Strike 7
6m	93.11	96.45	99.90	103.48	107.19	111.03	115.01
1y	87.69	92.19	96.93	101.91	107.15	112.66	118.45
3y	74.04	80.73	88.03	95.99	104.68	114.14	124.46
5y	64.64	72.28	80.84	90.40	101.09	113.05	126.42
7y	57.23	65.33	74.57	85.12	97.16	110.91	126.60
10y	48.42	56.71	66.42	77.80	91.12	106.73	125.02
15y	37.45	45.46	55.17	66.96	81.26	98.62	119.70
20y	29.46	36.84	46.08	57.62	72.06	90.12	112.70
25y	23.43	30.08	38.62	49.59	63.68	81.76	104.98
30y	18.77	24.68	32.45	42.68	56.12	73.80	97.05

TABLE 1. Expiries and strikes of FX options used in calibrating the model.

10. Test results

10.1. **The data.** Tests have been carried out for a standardized set of market data. The interest rate curves in the domestic (Japanese yen) and foreign (US dollar) economies are given by

$$\begin{aligned} P_d(0,T) &= \exp(-0.02 \times T), \\ P_f(0,T) &= \exp(-0.05 \times T). \end{aligned}$$

The volatility parameters for the interest rate evolution in both currencies are given by

$$\begin{aligned} \sigma_d(t) &\equiv 0.70\%, \quad \varkappa_d(t) \equiv 0.0\%, \\ \sigma_f(t) &\equiv 1.20\%, \quad \varkappa_f(t) \equiv 5.0\%. \end{aligned}$$

The correlation parameters are given by

$$\rho_{df} = 25.00\%, \quad \rho_{dS} = -15.00\%, \quad \rho_{fS} = -15.00\%.$$

The initial spot FX rate (yen per dollar) is set at 105.00. The expiries, $T_1, \dots, T_{10}$ considered, and the strikes $K_i(T_n)$ of options used in calibration, are given in Table 1.

Note that the strikes for each expiry T_n, $n = 1, \dots, 10$, are computed by using the formula

$$\begin{aligned} K_i(T_n) &= F(0,T_n) \exp\left(0.1 \times T_n^{1/2} \times \delta_i\right), \\ \delta_i &= -1.5, -1.0, -0.5, 0.0, 0.5, 1.0, 1.5. \end{aligned}$$

In particular, the strikes in column 4 ($K_4(T_n)$, $n = 1, \dots, 10$) are equal to forward FX rates to T_n.

For each expiry and strike, an implied Black volatility of the corresponding FX option is given in Table 2. This set of parameters is regarded as "the market".

For each expiry T_n, $n = 1, \dots, N$, we fit a displaced-diffusion model with a constant volatility σ_n^* and a constant skew parameter δ_n^*, $n = 1, \dots, 10$ (see Section 8 for notations). The skews are fitted to match the slopes of the market FX volatility smiles for each expiry, and the volatilities are fitted to the at-the-money volatilities. The resulting parameters are summarized in Table 3.

The cross-currency model is calibrated to these parameters, as outlined in Section 8. The resulting parameters ((ν_n, β_n), $n = 1, \dots, N$) are summarized in Table 4.

10.2. **Quality of approximation.** In this section, the errors in the approximation formulas from Theorem 7.2 are investigated. For the model from Section 10.1 (see Table 4 for the model parameters used), values of FX options with expiries/strikes given by Table 1 are computed using two methods. For the first method, the approximation formula from Theorem 7.2 is used. For the second method, a 3-dimensional PDE scheme (an ADI scheme from [CS88]) is used with 100 time steps, 150 FX steps, and 50 steps in each of the interest rate directions. The values from both methods are

Expiry	Vol 1	Vol 2	Vol 3	Vol 4	Vol 5	Vol 6	Vol 7
6m	11.41%	10.49%	9.66%	9.02%	8.72%	8.66%	8.68%
1y	12.23%	10.98%	9.82%	8.95%	8.59%	8.59%	8.65%
3y	12.94%	11.35%	9.89%	8.78%	8.34%	8.36%	8.46%
5y	13.44%	11.84%	10.38%	9.27%	8.76%	8.71%	8.83%
7y	14.29%	12.68%	11.23%	10.12%	9.52%	9.37%	9.43%
10y	16.43%	14.79%	13.34%	12.18%	11.43%	11.07%	10.99%
15y	20.93%	19.13%	17.56%	16.27%	15.29%	14.65%	14.29%
20y	22.96%	21.19%	19.68%	18.44%	17.50%	16.84%	16.46%
25y	23.97%	22.31%	20.92%	19.80%	18.95%	18.37%	18.02%
30y	25.09%	23.48%	22.17%	21.13%	20.35%	19.81%	19.48%

TABLE 2. Market implied Black volatilities of FX options for expiries and strikes from Table 1

Expiry	Volatility	Skew
6m	9.02%	-200%
1y	8.94%	-180%
3y	8.78%	-110%
5y	9.25%	-60%
7y	10.09%	-30%
10y	12.11%	0%
15y	16.03%	30%
20y	18.05%	50%
25y	19.32%	63%
30y	20.56%	72%

TABLE 3. Market (term) volatilities and skews (σ_n^*, δ_n^*), $n = 1, \ldots, 10$, of the displaced-difusion model, as calibrated to market-implied Black volatilities of FX options from Table 2 by matching the value and the slope of the FX volatility smile for each expiry.

Start period	End period	Volatility	Skew
0m	6m	9.03%	-200%
6m	1y	8.87%	-172%
1y	3y	8.42%	-115%
3y	5y	8.99%	-65%
5y	7y	10.18%	-50%
7y	10y	13.30%	-24%
10y	15y	18.18%	10%
15y	20y	16.73%	38%
20y	25y	13.51%	38%
25y	30y	13.51%	38%

TABLE 4. Model volatilities and skews (ν_n, β_n), $n = 1, \ldots, N$, as calibrated to the market ones from Table 3.

Expiry	Error 1	Error 2	Error 3	Error 4	Error 5	Error 6	Error 7
6m	-0.26%	-0.16%	-0.12%	-0.10%	-0.07%	-0.02%	0.05%
1y	-0.06%	-0.06%	-0.07%	-0.06%	-0.03%	0.03%	0.14%
3y	0.14%	0.07%	0.00%	-0.02%	0.01%	0.11%	0.28%
5y	0.17%	0.11%	0.04%	0.00%	0.03%	0.12%	0.30%
7y	0.21%	0.16%	0.07%	0.02%	0.03%	0.12%	0.29%
10y	0.19%	0.19%	0.11%	0.04%	0.03%	0.08%	0.20%
15y	-0.01%	0.08%	0.07%	0.01%	-0.04%	-0.08%	-0.09%
20y	-0.39%	-0.17%	-0.08%	-0.05%	-0.06%	-0.08%	-0.11%
25y	-0.62%	-0.31%	-0.15%	-0.06%	-0.03%	-0.02%	-0.02%
30y	-0.82%	-0.42%	-0.18%	-0.06%	0.02%	0.05%	0.06%

TABLE 5. Differences, in implied Black volatilities, between values of FX options computed using the PDE method and the approximation method from Theorem 7.2.

expressed in implied Black volatilities. The difference between the two sets of volatilities is reported in Table 5. The quality of approximation can also be visually assessed from Figures 1, 2, and 3. Clearly, the fit is excellent throughout, with errors less than 0.10% for at-the-money options, and less than 0.20% for almost all others. Slight deterioration of quality occurs for very long-dated (25 and 30 years) option with low strikes, which can be explained as follows. For the actual model (2.2), the zero FX rate point ($F = 0$) is an absorbing barrier (that may or may not be reachable depending on the values of the skew parameters). In the displaced-diffusion model used as an approximation in Theorem 7.2, FX rate can actually go negative (if the skew parameter is less than 1.0). This difference starts to matter for low strikes at long maturities.

10.3. **Fit to the market.** In this section we look at how well the model fits the market. The market is given by the implied Black volatilities in Table 2. We compute the values of FX options in the model (2.2) (with parameters given in Table 4) using the PDE method, and compare them to the market volatilities. The differences are reported in Table 6. Also, visual comparison between the market volatility smiles and the ones generated by the model calibrated to it, is presented in Figures 4, 5, and 6. Clearly, the calibration algorithm works as intended, with an excellent fit to the at-the-money options and to the slopes of volatility smiles for each expiry. The fit to individual FX options is not always perfect, which is more of a limitation of the model specification used (see Section 9) than the calibration algorithm. Still, the smiles produced by the model are much closer to the market than the ones generated by the log-normal model. In particular, the fit, compared to the log-normal model, is much better for low-strike (in-the-money call) options.

11. Skew impact on PRDCs

A power-reverse dual-currency swap, or PRDC, (see [SO02], [sto03] for extensive discussions) pays FX-linked coupons in exchange for floating-rate payments. Let us define it more formally[4]. Suppose, a tenor structure

$$0 < T_1 \cdots < \cdots < T_N,$$
$$\tau_n = T_{n+1} - T_n,$$

is given. An FX-linked, or PRDC, coupon for the period $[T_n, T_{n+1}]$, $n = 1, \ldots, N-1$, pays the amount

$$\tau_n C_n \left(S \left(T_n \right) \right)$$

[4]A large variety of PRDCs is available. We only present the basic structure, as relevant for our analysis.

Expiry	Error 1	Error 2	Error 3	Error 4	Error 5	Error 6	Error 7
6m	-1.19%	-0.64%	-0.24%	-0.05%	-0.20%	-0.58%	-1.03%
1y	-1.44%	-0.81%	-0.27%	-0.02%	-0.27%	-0.85%	-1.46%
3y	-1.57%	-0.86%	-0.26%	0.02%	-0.30%	-1.03%	-1.79%
5y	-1.39%	-0.71%	-0.19%	0.05%	-0.24%	-0.92%	-1.67%
7y	-1.15%	-0.54%	-0.11%	0.06%	-0.18%	-0.77%	-1.47%
10y	-0.81%	-0.29%	0.01%	0.09%	-0.13%	-0.63%	-1.27%
15y	-0.72%	-0.24%	0.02%	0.06%	-0.11%	-0.49%	-1.03%
20y	-0.94%	-0.40%	-0.10%	0.00%	-0.10%	-0.37%	-0.80%
25y	-1.00%	-0.45%	-0.13%	0.00%	-0.06%	-0.26%	-0.60%
30y	-1.12%	-0.52%	-0.16%	0.00%	0.00%	-0.14%	-0.40%

TABLE 6. Differences, in implied Black volatilities, between values of FX options valued in the model and their market values.

(on a unit notional in domestic currency) at time T_n, where

$$C_n(S) = \min\left(\max\left(g_f \frac{S(T_n)}{s} - g_d, b_l\right), b_u\right), \quad n = 1, \ldots, N-1.$$

Quantities g_f and g_d are called the *foreign* and the *domestic* coupons, and b_l and b_u are the *floor* and the *cap* on the payoff. In the classical structure, $b_l = 0$ and $b_u = +\infty$, ie the payoff is floored at zero and there is no cap. The scaling factor s is often called the *initial FX rate*. All the parameters can vary from coupon to coupon, ie depend on n, $n = 1, \ldots, N-1$.

An initial fixed-rate coupon is often paid to the investor (the receiver of PRDC coupons). It is not included in the definition above as its valuation is straightforward.

With the domestic currency being the Japanese yen, and the foreign one being the US dollar, $S(\cdot)$ is expressed in yen per dollar. The investor receives a positive coupon as long as $S(\cdot)$ is high, ie as long as the dollar is strong (or strong enough). Because of the significant interest rate differential between the two currencies, the forward FX rate curve $F(0,t)$, $t \geq 0$, is strongly downward sloping, predicting a significant weakening of the dollar. Thus, the party receiving the structured coupon in a PRDC is essentially betting that the dollar is not going to weaken (or not as much) as predicted by the forward FX curve, a bet that many Japanese investors are comfortable to make.

The standard PRDC swap can be seen as a collection of simple FX options, and as such does not require a sophisticated model to price. The varieties that are most popular, however, are more complicated and do require a model. One type, a cancellable PRDC, gives the issuer (the payer of the PRDC coupons) the right to cancel the swap on any of the dates $T_1, \ldots, T_{N-1}$ (or a subset thereof). The other popular type is a knockout PRDC, stipulating that the swap knocks out (disappears) if the spot FX rate on any of the dates $T_1, \ldots, T_{N-1}$ exceeds a pre-agreed upon level. Both features are designed to limit the downside for the issuer, and also allow the investor to monetize the options to cancel/knockout in the form of receiving high fixed coupons over the initial (no-call) period $[0, T_1]$.

Assuming $b_u = +\infty$, $b_l = 0$ (most commonly used settings), the PRDC coupon can be represented as a call option on the FX rate,

$$C_n(S) = h \max(S(T_n) - k, 0), \quad k = \frac{s g_d}{g_f}, \quad h = \frac{g_f}{s}.$$

The *option notional* h determines the overall level of coupon payment, and the strike k determines the likelihood of the coupon paying a non-zero amount. The relationship of the strike to the forward FX rate to T_n determines the *leverage* of the PRDC. If the strike k is low, then the coupon has a relatively-high chance of paying a non-zero amount. The option notional in this case is, typically,

Leverage	Low	Medium	High
Trade details			
Foreign coupon	4.50%	6.25%	9.00%
Domestic coupon	2.25%	4.36%	8.10%
Barrier	110.00	120.00	130.00
PV, lognormal model			
Underlying	-8.66	-9.24	-9.35
Cancellable	13.61	17.13	23.16
Knockout	4.16	8.08	14.12
PV, skew model			
Underlying	-10.67	-11.66	-10.86
Cancellable	11.90	14.62	20.37
Knockout	1.52	2.89	6.32
Diff, skew - lognormal			
Underlying	-2.01	-2.43	-1.52
Cancellable	-1.71	-2.51	-2.79
Knockout	-2.64	-5.19	-7.80

TABLE 7. Parameters of PRDCs (the underlying swap, the cancellable and the FX knockout variants) and their values, in percentage points of the notional using the standard log-normal model and the skew-calibrated model.

low. This is a low-leverage situation. If the strike is high relative to the forward FX rate, that the probability that the coupon will pay a non-zero amount is low. The notional h, in this case, is typically higher. This is a high-leverage situation.

In the analysis below, PRDCs of different leverage are used to demonstrate the smile impact. We consider cancellable and knockout versions of three PRDC swaps, a low-leverage, a medium-leverage, and a high-leverage one. The three swaps share many features in common, namely

- They start in 1 year ($T_1 = 1$) and have total maturity of 30 years ($T_N = 30$);
- All pay an annual PRDC coupon ($\tau_n = 1$, $n = 1, \dots, N-1$) and receive the domestic (yen) Libor rate;
- The floor is zero and there is no cap, $b_l = 0$, $b_u = +\infty$;
- All have a time-dependent schedule of $s = s_n$; in particular,

$$s_n = F(0, T_n), \quad n = 1, \dots, N-1;$$

  This choice simplifies the structure of coupons, clarifying certain conclusions.
- Cancellable variants give a Bermuda-style option to cancel the swap on each of the dates $T_1, \dots, T_{N-1}$ to the payer of the PRDC coupons;
- Knockout variants are up-and-out FX-linked barriers. In particular, the swap disappears on the first date among $T_1, \dots, T_{N-1}$ on which the FX rate $S(T_n)$ exceeds a given barrier. Note that the barriers are different for the three cases.

The domestic and foreign coupons are chosen to provide different amounts of leverage, while keeping the total value of the underlying swap roughly the same for all three cases. Table 7 provides the remaining details of the securities.

The values of securities are in percentage points of the notional. Valuation results for two models are presented. One is the standard log-normal 3-factor model, ie (2.2) with $\gamma(t, x)$ (see (2.4)) independent of x, and calibrated to the at-the-money FX options of expiries from Table 1. The other model is the skew-calibrated one as described above. The values (to the payer of PRDC coupons) of underlying PRDC swaps, cancellable PRDCs and knockout PRDCs are reported.

First, let us consider the effect of leverage on the values of securities. The PRDC coupon strike (k) for the low-leverage swap is set at 50% of the forward FX rate for the appropriate expiry. It is 70% for the medium-leverage swap, and 90% for the high-leverage swap. All underlying swaps have roughly the same value under the log-normal model. However, the value of cancellable and knockout swaps increases with leverage. This is of course not surprising, as higher volatility in the value of the underlying swap (resulting from higher leverage) increases the value of the option to cancel it (and the knockout option in this case). The values of cancellable swaps indicate the level of the initial fixed coupon that the issuer is willing to pay to the investor. For a low-leverage swap (under the log-normal model), the issuer can pay up to 13.61% net coupon in the first year and still have a positive PV of his position (of course, he is likely to pay less, booking the rest as profit and/or reserves). For the high-leverage swap, the issuer can pay up 23.16% net coupon to the investor. Both, of course, are extremely attractive to yield-deprived Japanese investors, but the higher-leverage cancellable swap naturally provides a more attractive initial coupon.

Next, let us consider the effect of introducing the skew on the underlying PRDC swaps. PRDC swaps consist of (short) FX call options with low strikes ("low" means "weak dollar" for the analysis in this section). Analyzing Figures 1, 2 and 3, it becomes clear that introduction of the skew *increases* the implied volatility of low-strike options, thus pushing the value of PRDCs *down* (for the issuer). Interestingly, the effect is the most pronounced for medium-leverage swaps. The reason is that the total effect is a combination of the change in impled volatilities, and the level of sensitivities of the options to those changes. The volatilities change the most for low-leverage swaps because the PRDC coupon strikes are the lowest. Low-strike options, however, have the lowest sensitivity (Vega) to volatility. The situation is reversed for high-leverage swaps. The volatilities change little, but the sensitivity to the changes is high. The combined effect is the strongest for medium-leverage swaps.

Now let us look at cancellable swaps. The (negative) impact can be seen uniformly increasing with the increased leverage. The effect is quite substantial, between -1.70% to -2.80%. The impact is even more pronounced on knockouts, with the values changing by the amounts ranging from -2.60% to -7.80%. These changes in values are comparable to typical profits booked by the issuer. Hence, not accounting for the FX skew can easily show a profit on a trade that was actually a loss. The conclusion is not surprising: *accounting for the FX skew, for example in the way developed in this paper, is absolutely critical for proper pricing and risk-managing the PRDC book.*

The FX skew impact on the underlying PRDC swaps is easy to understand, as the swaps are just collections of simple FX options. Corresponding analysis for cancellable and knockouts is harder because of their more complicated structure. To aid in understanding the forces at work, let us look at the value of a cancellable PRDC at an intermediate date as a function of the spot FX rate on that date. For the purposes of this qualitative analysis, the interest rate factors are assumed to have no volatility. The appropriate payoff (for the high-leverage cancellable PRDC in $T = 5$ years) is presented in Figure 7. The value is, as always, from the point of view of the issuer. Clearly, it is optimal to cancel the swap if the FX rate is high enough (above about 135 yen per dollar for the cancel opportunity in $T = 5$ years). The forward FX rate for $T = 5$ is about 90. The payoff is concave for $S < 90$, reflecting the negative convexity of short FX option positions, the PRDC coupons due to the issuer. For $S > 90$, the payoff is convex, reflecting the cancel option at higher strike. In particular, accounting for the skew affects the value of a cancellable in two ways. First, the higher volatility for lower strikes means that the "left", concave, side of the payoff is valued *lower*. The lower volatility for high strikes means that the "right", convex side of the payoff is also valued *lower*. Hence, the skew impact on cancellable PRDCs is *compounded*. The profile of the cancellable PRDC is similar to a call spread, a payoff that is very sensitive to the skew of the volatility smile. With the model developed in this paper, the skew of the smile can be nicely

controlled, thus allowing to capture the main risk factors affecting these types of securities very well.

Incidentally, the profile of a knockout PRDC is similar to that of a cancellable PRDC, as it goes to zero for high values of the FX rate. The extra sensitivity of knockout PRDCs to the skew comes from the fact that the payoff is in fact discontinuous at the boundary, unlike for the cancellable. Digital-like options are also known to be primarily affected by the slope of the FX smile.

Another approach to understanding the exposures of a PRDC to changes in the shapes of volatility smiles is by means of analyzing its FX Vega profile, ie the dependence of FX Vega on the spot FX rate. The FX Vega is defined as the sensitivity of the value to (parallel) shifts of the at-the-money FX volatilities. Figure 8 presents such a profile for a cancellable PRDC. The graph confirms the volatility skew analysis above in that as low-strike volatilities are increased, or high-strike volatilities are decreased, the value of the cancellable PRDC goes down, since the Vega on the "left" side of the graph is negative, and on the "right" side it is positive.

The particular shape of the exposure of cancellable and knockout PRDCs to FX volatilities make it impossible to reproduce the impact of the FX volatility smile on valuation within a less-flexible model such as the log-normal model discussed above. While it is often possible to introduce the smile effect into valuation by judiciously choosing the strikes of (in this case) FX options to which to calibrate the log-normal model to, it clearly will not work for PRDCs, as there is no single strike to encapsulate the required dependence. One cannot find the "effective" strike, as it is the slope of the FX volatility smile that matters.

12. Conclusions

A model that explicitly incorporates the FX volatility smile into a multi-dimensional, cross-currency model suitable for valuation of power-reverse dual-currency securities is developed. In particular, a procedure for calibrating the model to the FX volatility smiles for all expiries is presented. It is based on a Markovian representation of the dynamics of the forward FX rate, combined with powerful skew averaging techniques, and is essentially instantaneous. The FX-skew-enabled model is an extension of the standard three-factor log-normal model and, with the calibration procedure presented here, shares all of its advantages including the speed of valuation and simplicity of calibration. It is, however, much more flexible in its fit to FX options across multiple expiries.

The effect of FX volatility skew on PRDCs (cancellable and knockout varieties) is studied, and is found significant. In particular, by analyzing the shapes of the payoffs of the securities, it is determined that the slope of the FX volatility smile is a major factor affecting the values. While the model is not very flexible in reproducing the convexity of FX volatility smiles observed in the market, the ability to control the slope of the smile within the model is thus particularly important.

References

[AA02] Leif B.G. Andersen and Jesper Andreasen. Volatile volatilities. *Risk*, 15(12), December 2002.

[ABOBF02] Marco Avellaneda, Dash Boyer-Olson, Jérôme Busca, and Peter Friz. Reconstructing volatility. *Risk*, 15(10), October 2002.

[Bal05] Philippe Balland. Stochastic volatility for hybrids. World Business Strategies workshop on hybrids, 2005.

[BM01] D. Brigo and F. Mercurio. *Interest-Rate Models - Theory and Practice*. Springer Verlag, 2001.

[CS88] J. J. D. Craig and A. D. Sneyd. An alternating-direction implicit scheme for parabolic equations with mixed derivatives. *Comput. Math. Appl.*, 16(4):341–350, 1988.

[DH97] M.A.H. Dempster and J.P. Hutton. Numerical valuation of cross-currency swaps and swaptions. In M.A.H. Dempster and S.R. Pliska, editors, *Mathematics of derivative securities*, pages 473–503. Cambridge University Press, 1997.

[Dup94] Bruno Dupire. Pricing with a smile. *Risk*, 7(1), January 1994.

[KS97] Ioannis Karatzas and Steven E. Shreve. *Brownian Motion and Stochastic Calculus*. Springer, 1997.

[Pit05a] Vladimir V. Piterbarg. A stochastic volatility model with time-dependent skew. To appear in Applied Mathematical Finance, 2005.

[Pit05b] Vladimir V. Piterbarg. Time to smile. To appear in Risk Magazine, 2005.
[SO02] Jason Sippel and Shoichi Ohkoshi. All power to PRDC notes. *Risk*, 15(11), October 2002.
[sto03] Cover story. The problem with power-reverse duals. *Risk*, 16(10), October 2003.

Appendix A. Proof of Theorem 6.1

Recall the definition

$$c(t,T,K) = P_d(0,t)\,\mathbf{E}_0^T\left((F(t,T)-K)^+\right).$$

The local volatility $\tilde{\Lambda}(t,x)$ such that the values of European options in the model

$$\frac{dF(t,T)}{F(t,T)} = \tilde{\Lambda}(t,F(t,T))\,dW_F(t)$$

match $\{c(,T,K)\}_{t,K}$ is given by the well-known result by Dupire (see [Dup94]),

$$\left(K\tilde{\Lambda}(t,K)\right)^2 = 2\frac{\frac{\partial}{\partial t}\frac{c(t,T,K)}{P_d(0,t)}}{\frac{\partial^2}{\partial K^2}\frac{c(t,T,K)}{P_d(0,t)}}. \tag{A.1}$$

To compute the right-had side, we first write (the use of delta-functions in the integrands can be rigorously justified by Tanaka's formula, see [KS97])

$$d(F(t,T)-K)^+ = 1_{\{F(t,T)>K\}}dF(t,T) + \frac{1}{2}\delta_{\{F(t,T)=K\}}d\langle F(t,T)\rangle,$$

and, since $F(t,T)$ is a martingale under the domestic T-forward measure,

$$\mathbf{E}^T(F(t,T)-K)^+ - (F(0,T)-K)^+ = \frac{1}{2}\int_0^t \mathbf{E}^T\left(\delta_{\{F(t,T)=K\}}d\langle F(t,T)\rangle\right).$$

Clearly

$$\mathbf{E}^T\left(\delta_{\{F(t,T)=K\}}d\langle F(t,T)\rangle\right) = \mathbf{E}^T\left(\delta_{\{F(t,T)=K\}}\right)\times\mathbf{E}^T\left(d\langle F(t,T)\rangle\middle|\,F(t,T)=K\right)$$

and

$$\mathbf{E}^T\left(\delta_{\{F(t,T)=K\}}\right) = \frac{\partial^2}{\partial K^2}\mathbf{E}^T(F(t,T)-K)^+ = \frac{\partial^2}{\partial K^2}\frac{c(t,T,K)}{P_d(0,t)}.$$

Moreover, by Proposition 5.1,

$$d\langle F(t,T)\rangle = F^2(t,T)\,\Lambda^2(t,F(t,T)D(t,T))\,dt,$$

so that

$$\mathbf{E}^T\left(\delta_{\{F(t,T)=K\}}d\langle F(t,T)\rangle\right) = \frac{\partial^2}{\partial K^2}\frac{c(t,T,K)}{P_d(0,t)}\times K^2\times\mathbf{E}^T\left(\Lambda^2(t,F(t,T)D(t,T))\middle|\,F(t,T)=K\right)dt.$$

In particular,

$$\begin{aligned}\frac{\partial}{\partial t}\frac{c(t,T,K)}{P_d(0,t)} &= \frac{\partial}{\partial t}\left(\mathbf{E}^T(F(t,T)-K)^+ - (F(0,T)-K)^+\right)\\ &= \frac{1}{2}\times\frac{\partial^2}{\partial K^2}\frac{c(t,T,K)}{P_d(0,t)}\times K^2\times\mathbf{E}^T\left(\Lambda^2(t,F(t,T)D(t,T))\middle|\,F(t,T)=K\right).\end{aligned}$$

Substituting this equality into (A.1) we obtain

$$\tilde{\Lambda}^2(t,K) = \mathbf{E}^T\left(\Lambda^2(t,F(t,T)D(t,T))\middle|\,F(t,T)=K\right),$$

and the theorem is proved.

Appendix B. Proof of Corollary 6.2

The proof is based on Theorem 6.1 and the following lemma.

Lemma B.1. *For any $c \in \mathbb{R}$,*

$$\mathbf{E}^T\left(\left(D\left(t,T\right)\right)^c \middle| F\left(t,T\right)=x\right) \approx \left(D_0\left(t,T\right)\right)^c \left(1 + c \times \frac{\int_0^t \chi_{Z,F}\left(s\right)\, ds}{\int_0^t \chi_{F,F}\left(s\right)\, ds} \times \left(\frac{x}{F\left(0,T\right)} - 1\right)\right),$$

where $\chi_{Z,F}\left(t\right)$, $\chi_{F,F}\left(t\right)$ are defined by (6.5).

Proof. Under the domestic T-forward measure,

$$dP_d\left(t,T\right)/P_d\left(t,T\right) = \left(r_d\left(t\right) + \sigma_d^2\left(t,T\right)\right)\, dt + \sigma_d\left(t,T\right)\, dW_d^T\left(t\right),$$
$$dP_f\left(t,T\right)/P_f\left(t,T\right) = \left(r_f\left(t\right) + \rho_{fS}\sigma_f\left(t,T\right)\gamma\left(t,S\left(t\right)\right) + \rho_{df}\sigma_f\left(t,T\right)\sigma_d\left(t,T\right)\right)\, dt + \sigma_f\left(t,T\right)\, dW_f^T\left(t\right).$$

Hence

$$\begin{aligned} dD\left(t,T\right)/D\left(t,D\right) = &\left(r_d\left(t\right) - r_f\left(t\right)\right)\, dt \\ &- \rho_{fS}\sigma_f\left(t,T\right)\gamma\left(t,S\left(t\right)\right)\, dt \\ &+ \left(\sigma_d^2\left(t,T\right) - 2\rho_{df}\sigma_f\left(t,T\right)\sigma_d\left(t,T\right) + \sigma_f^2\left(t,T\right)\right)\, dt \\ &+ \sigma_d\left(t,T\right)\, dW_d^T\left(t\right) - \sigma_f\left(t,T\right)\, dW_f^T\left(t\right). \end{aligned}$$

By approximating $r_d\left(t\right)$, $r_f\left(t\right)$ "along the forward",

$$r_i\left(t\right) \approx -\left.\frac{\partial}{\partial T}\log P_i\left(0,t,T\right)\right|_{T=t}, \quad i = d, f,$$

and ignoring the drift terms that are quadratic in volatility, the following expression is obtained,

$$\begin{aligned} D\left(t,T\right) &\approx D_0\left(t,T\right) Z\left(t,T\right), \\ Z\left(t,T\right) &\triangleq \exp\left(\int_0^t \sigma_d\left(s,T\right)\, dW_d^T\left(s\right) - \int_0^t \sigma_f\left(s,T\right)\, dW_f^T\left(s\right)\right). \end{aligned}$$

Hence

$$\mathbf{E}^T\left(\left(D\left(t,T\right)\right)^c \middle| F\left(t,T\right)=x\right) = \left(D_0\left(t,T\right)\right)^c \mathbf{E}^T\left(\left(Z\left(t,T\right)\right)^c \middle| F\left(t,T\right)=x\right)$$

To compute $\mathbf{E}^T\left(\left(Z\left(t,T\right)\right)^c \middle| F\left(t,T\right)=x\right)$, a further Gaussian approximation is employed

$$\begin{aligned} \left(Z\left(t,T\right)\right)^c &\approx 1 + c\int_0^t \left[\sigma_d\left(s,T\right)\, dW_d^T\left(s\right) - \sigma_f\left(s,T\right)\, dW_f^T\left(s\right)\right], \\ F\left(t,T\right) &\approx F\left(0,T\right)\left(1 + \int_0^t \left[\sigma_f\left(t,T\right)\, dW_f^T\left(t\right) - \sigma_d\left(t,T\right)\, dW_d^T\left(t\right) + \gamma\left(t, F\left(0,T\right) D_0\left(t,T\right)\right) dW_S^T\left(t\right)\right]\right). \end{aligned}$$

Then

$$\mathbf{E}^T\left(\left(Z\left(t,T\right)\right)^c \middle| F\left(t,T\right)=x\right) \approx 1 + \frac{\left\langle \left(Z\left(t,T\right)\right)^c, F\left(t,T\right)\right\rangle}{\left\langle F\left(t,T\right), F\left(t,T\right)\right\rangle}\left(x - F\left(0,T\right)\right),$$

where

$$\begin{aligned} \left\langle \left(Z\left(t,T\right)\right)^c, F\left(t,T\right)\right\rangle &\approx cF\left(0,T\right)\int_0^t \chi_{Z,F}\left(s\right) ds, \\ \left\langle F\left(t,T\right), F\left(t,T\right)\right\rangle &\approx F^2\left(0,T\right)\int_0^t \chi_{F,F}\left(s\right) ds, \end{aligned}$$

and the definitions (6.5) are used. ∎

Recall Theorem 6.1 that states that for the purposes of computing European option values, the dynamics of the forward FX rate can be assumed to follow

$$\frac{dF(t,T)}{F(t,T)} = \tilde{\Lambda}(t, F(t,T))\, dW_F(t),$$

where

$$\tilde{\Lambda}^2(t,x) = \mathbf{E}^T\left(\Lambda^2(t, F(t,T) D(t,T))\middle| F(t,T) = x\right).$$

The corollary is proved by applying Lemma B.1 to approximate the value of the conditional expected value on the right-had side of this expression. We have, from Proposition 5.1, that

$$\Lambda^2(t,x) = a(t) + b(t)\gamma(t,x) + \gamma^2(t,x).$$

Then

$$\tilde{\Lambda}^2(t,x) = a(t) + b(t)\,\mathbf{E}^T\left(\gamma^2(t, F(t,T) D(t,T))\middle| F(t,T) = x\right) + \mathbf{E}^T\left(\gamma^2(t, F(t,T) D(t,T))\middle| F(t,T) = x\right)$$

Let us define

$$\tilde{\gamma}(t,x) \triangleq \mathbf{E}^T\left(\gamma(t, F(t,T) D(t,T))\middle| F(t,T) = x\right),$$

and approximate

$$\mathbf{E}^T\left(\gamma^2(t, F(t,T) D(t,T))\middle| F(t,T) = x\right) \approx \tilde{\gamma}^2(t,x),$$

so that

$$\tilde{\Lambda}^2(t,x) \approx a(t) + b(t)\tilde{\gamma}(t,x) + \tilde{\gamma}^2(t,x).$$

Using the form (2.4) of $\gamma(t,x)$, we obtain

$$\tilde{\gamma}(t,x) = \nu(t)\left(\frac{F(t,T)}{L(t)}\right)^{\beta(t)-1}\mathbf{E}^T\left((D(t,T))^{\beta(t)-1}\middle| F(t,T) = x\right).$$

Denoting

$$\begin{aligned}
\hat{\gamma}(t,x) &= (D_0(t,T))^{\beta(t)-1}\left(1 + (\beta(t)-1)\times\frac{\int_0^t \chi_{Z,F}(s)\, ds}{\int_0^t \chi_{F,F}(s)\, ds}\times\left(\frac{x}{F(0,T)} - 1\right)\right),\\
\hat{\Lambda}^2(t,x) &= a(t) + b(t)\hat{\gamma}(t,x) + \hat{\gamma}^2(t,x),
\end{aligned}$$

The corollary is proved by an application of Lemma B.1 with $c = \beta(t) - 1$.

Appendix C. Proof of Theorem 7.2

Let us apply Proposition 7.1 to

$$\begin{aligned}
g(t,x) &= x\hat{\Lambda}(t,x),\\
\bar{g}(x) &= \delta_F\frac{x}{F(0,T)} + (1-\delta_F),\\
X_0 &= F(0,T).
\end{aligned}$$

Then

$$\frac{\partial}{\partial x}\bar{g}(x)\Big|_{x=X_0} = \frac{\delta_F}{F(0,T)}.$$

Also,

$$\begin{aligned}\frac{\partial}{\partial x}g(t,x) &= \hat{\Lambda}(t,x) + x\frac{\partial}{\partial x}\hat{\Lambda}(t,x)\\ &= \hat{\Lambda}(t,x) + x\frac{\partial}{\partial x}\left(\left(a(t) + b(t)\hat{\gamma}(t,x) + \hat{\gamma}^2(t,x)\right)^{1/2}\right)\\ &= \hat{\Lambda}(t,x) + x\frac{b(t)\frac{\partial}{\partial x}\hat{\gamma}(t,x) + 2\hat{\gamma}(t,x)\frac{\partial}{\partial x}\hat{\gamma}(t,x)}{2\left(a(t) + b(t)\hat{\gamma}(t,x) + \hat{\gamma}^2(t,x)\right)^{1/2}}.\end{aligned}$$

In particular,

$$\frac{\frac{\partial}{\partial x}g(t,x)\big|_{x=X_0}}{g(t,x)} = \frac{1}{F(0,T)} + \frac{b(t)\eta(t) + 2\hat{\gamma}(t,F(0,T))\eta(t)}{2F(0,T)\hat{\Lambda}^2(t,F(0,T))},$$

where

$$\eta(t) = F(0,T)\left.\frac{\partial}{\partial x}\hat{\gamma}(t,x)\right|_{x=F(0,T)}.$$

By the result of Proposition 7.1 we have

$$\frac{\delta_F}{F(0,T)} = \int_0^T \left(\frac{1}{F(0,T)} + \frac{b(t)\eta(t) + 2\hat{\gamma}(t,F(0,T))\eta(t)}{2F(0,T)\hat{\Lambda}^2(t,F(0,T))}\right) w(t)\, dt,$$

and the expression (7.1) for δ_F follows. The rest of the theorem follows from the standard results on displaced-diffusion SDEs.

Appendix D. Figures

XXX

E-mail address: piterbarg@yahoo.com

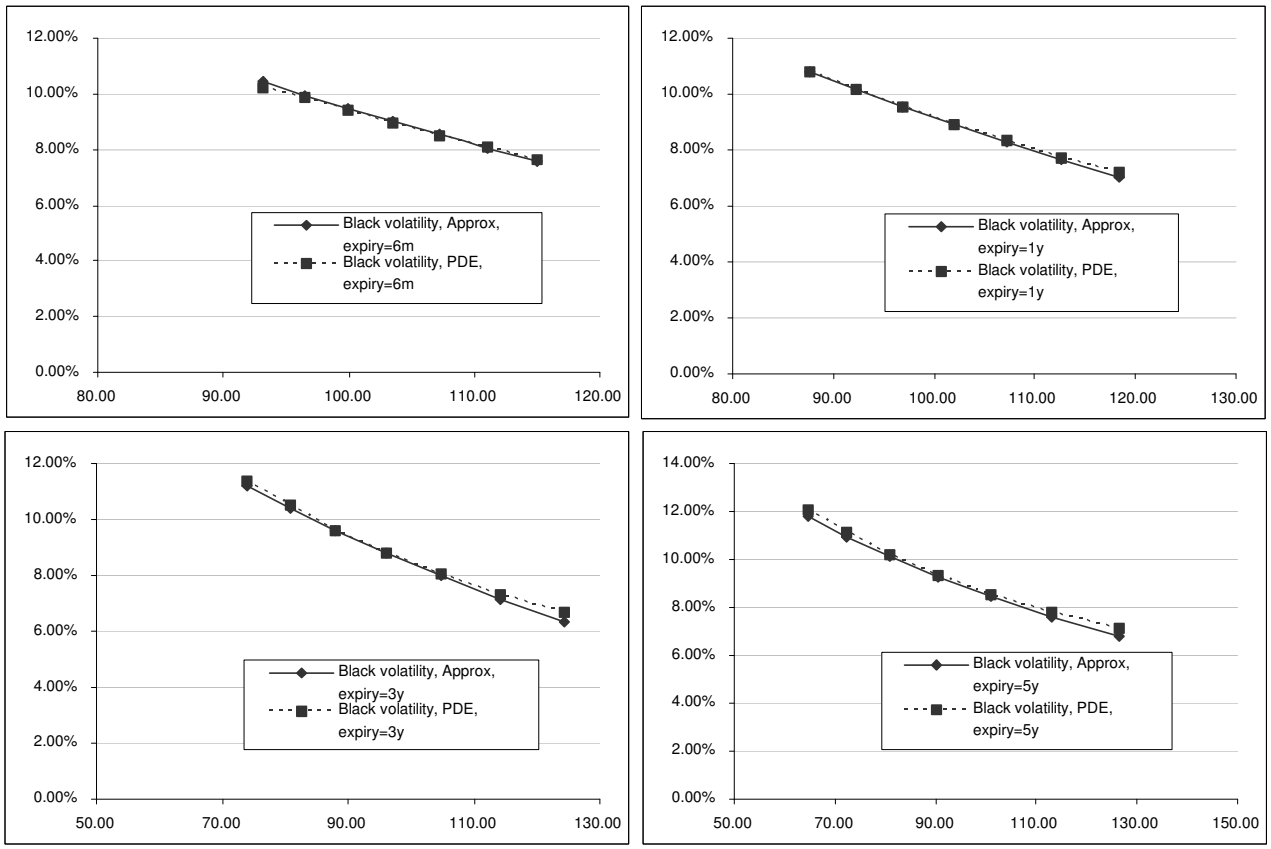

FIGURE 1. Black volatilities implied from FX option values computed using the PDE method and the approximation method of Theorem 7.2, versus FX option strike, for various option expiries.

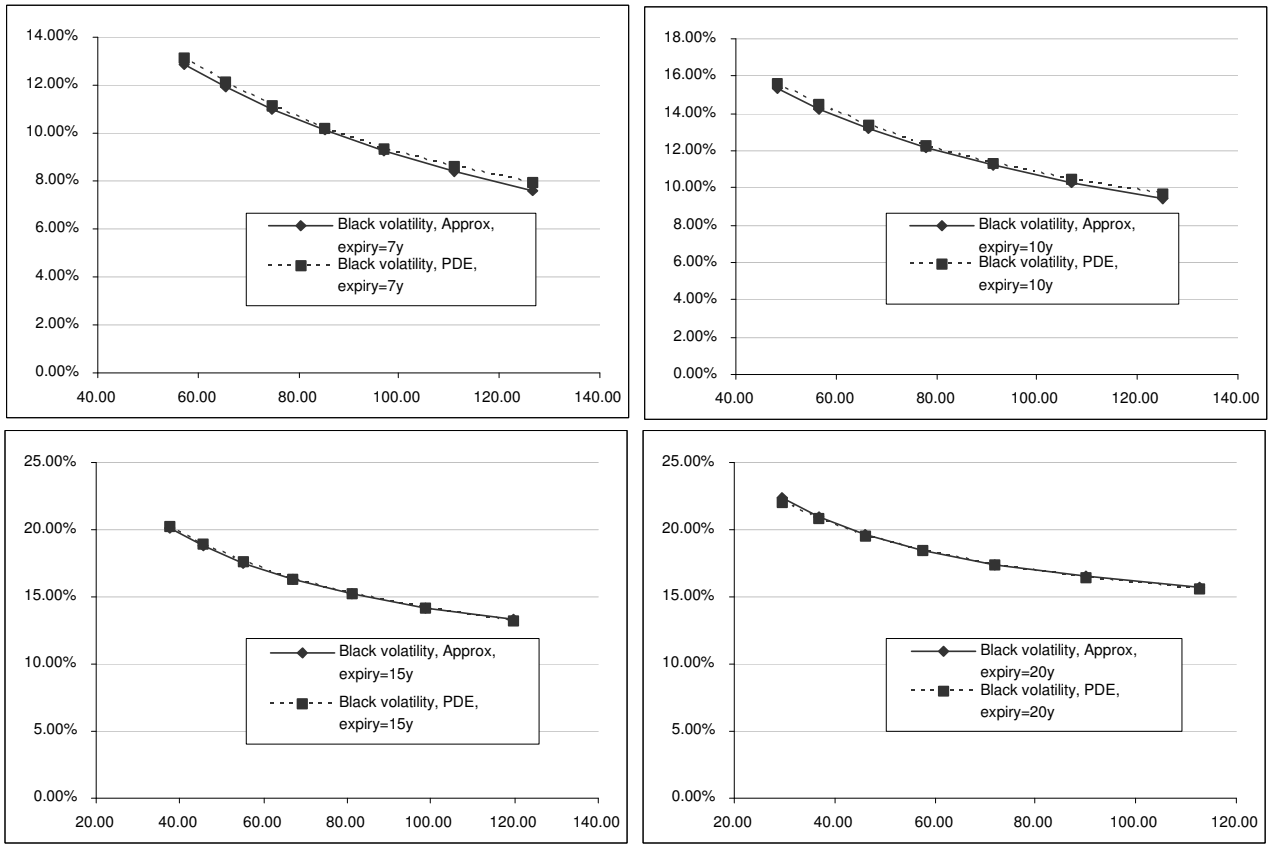

FIGURE 2. Black volatilities implied from FX option values computed using the PDE method and the approximation method of Theorem 7.2, versus FX option strike, for various option expiries.

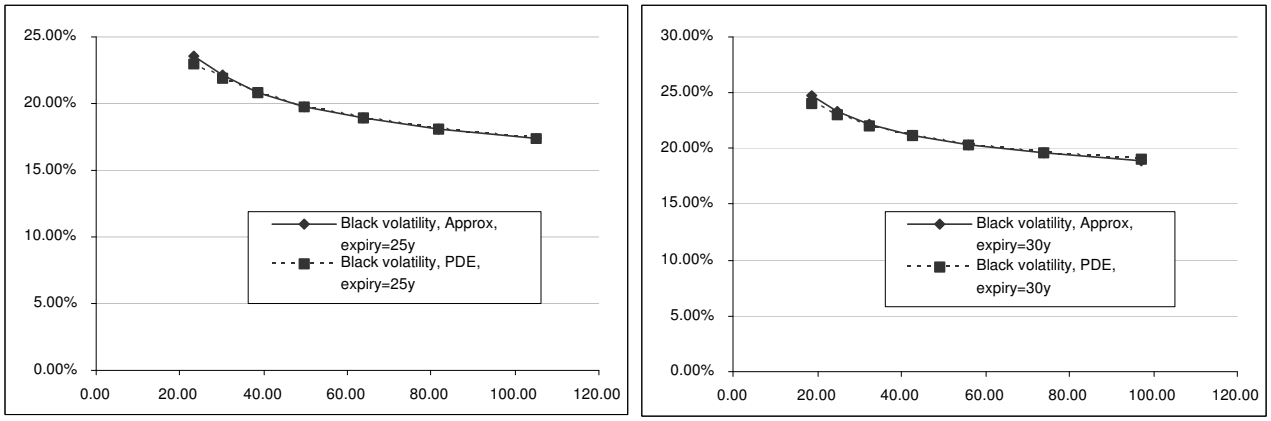

FIGURE 3. Black volatilities implied from FX option values computed using the PDE method and the approximation method of Theorem 7.2, versus FX option strike, for various option expiries.

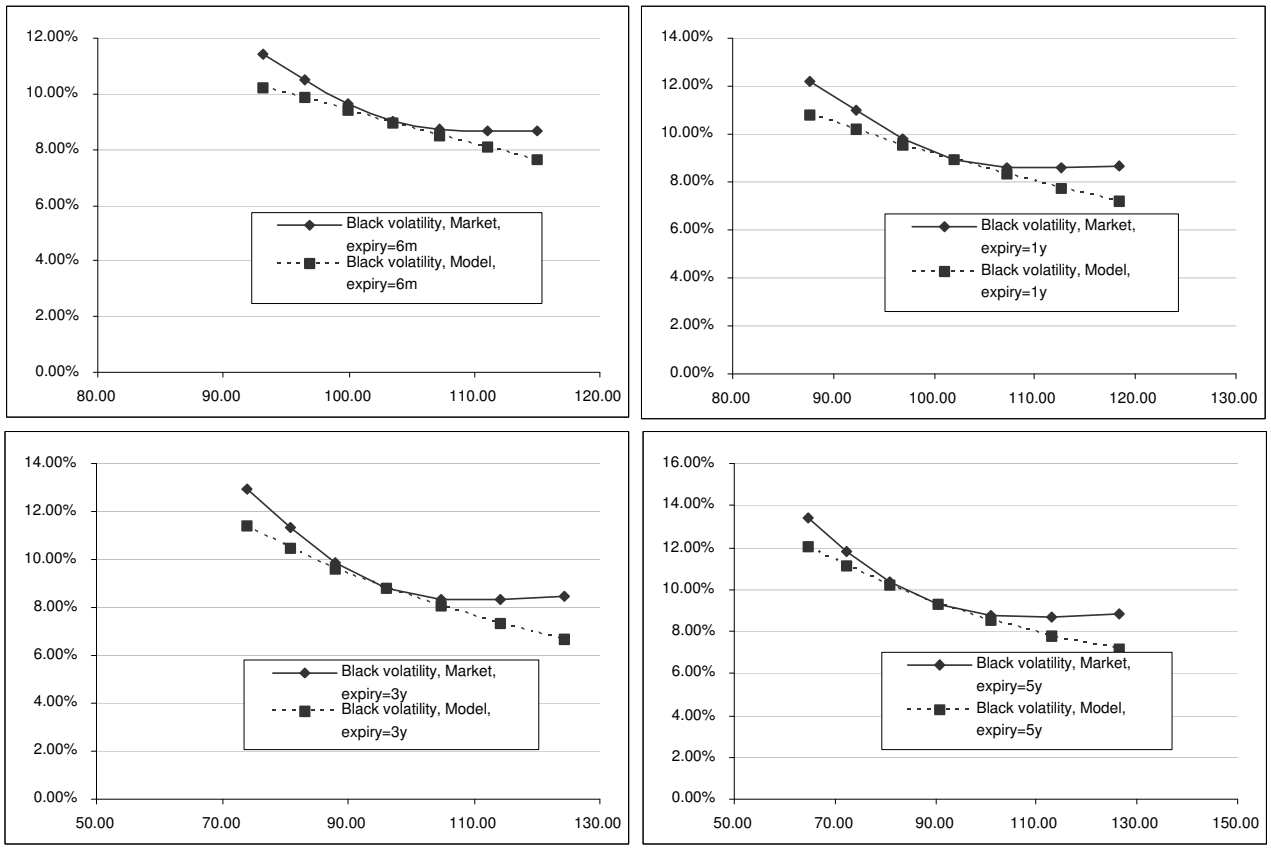

FIGURE 4. Market and model values of FX options, in implied Black volatilities, versus strikes, for a number of expiries.

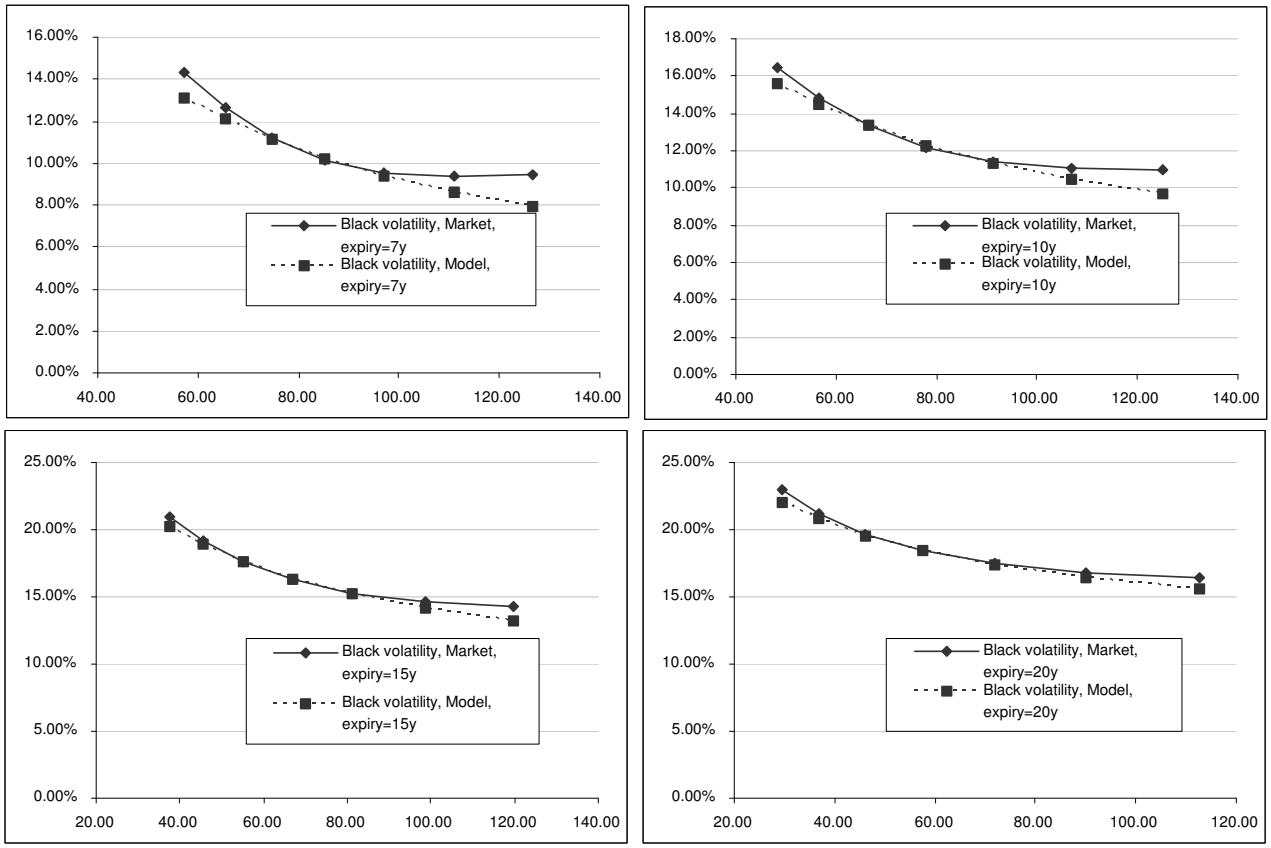

FIGURE 5. Market and model values of FX options, in implied Black volatilities, versus strikes, for a number of expiries.

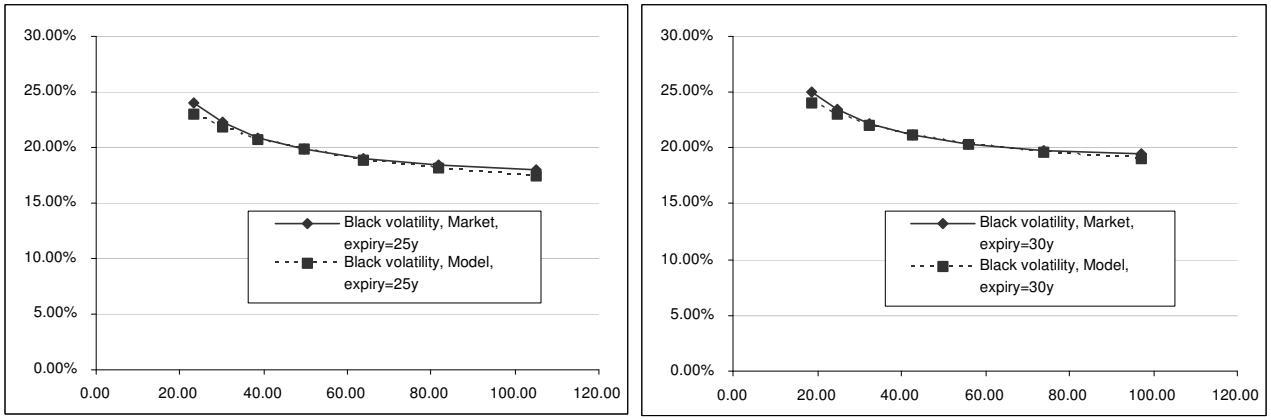

FIGURE 6. Market and model values of FX options, in implied Black volatilities, versus strikes, for a number of expiries.

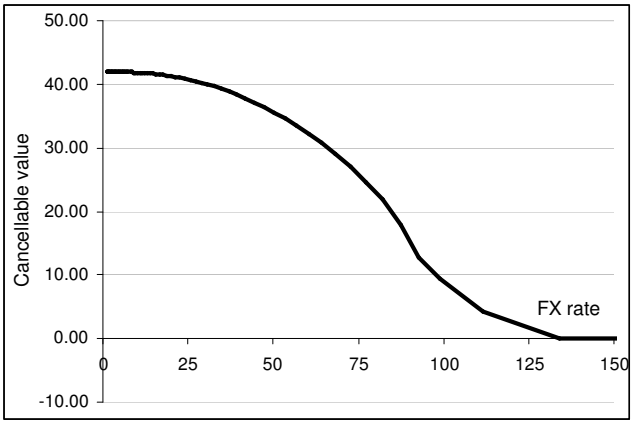

FIGURE 7. The value of a cancellable PRDC as a function of the FX rate at $T = 5$. The value in percentage points of the notional.

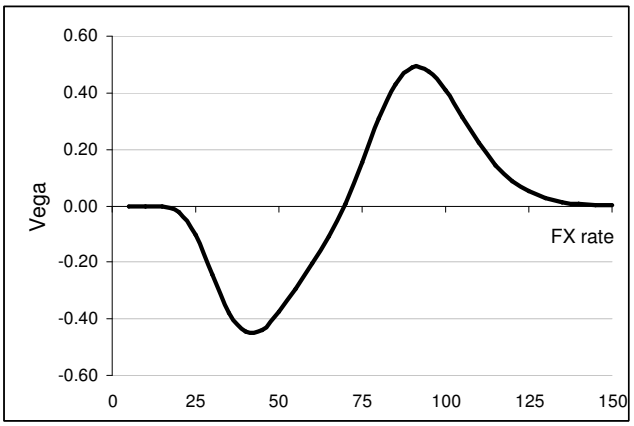

FIGURE 8. The vega (sensitivity to volatility, per 1% of the parallel shift in the at-the-money FX volatilities) of the cancellable PRDC, as a function of the spot FX rate.